Engineering Transactions, **71**(4): 617–644, 2023, doi: 10.24423/EngTrans.3114.20231121
Institute of Fundamental Technological Research Polish Academy of Sciences (IPPT PAN)
Université de Lorraine • Poznan University of Technology

Research Paper

Forced Nonlinear Vibrations in a Smart Magneto-Viscoelastic Multiscale Composite Nanobeam in a Humid Thermal Environment

Lakshmanan ANITHA[1)], Loganathan RAJALAKSHMI[2)],
Rajendran SELVAMANI[3)*], Farzad EBRAHIMI[4)]

[1)] *Department of Mathematics, Nehru Memorial College*
Puthanampatti, Trichy, Tamilnadu, India; e-mail: anithal@nmc.ac.in

[2)] *Department of Mathematics, Nandha Arts and Science College*
Erode, Tamilnadu, India; e-mail: lraji.028@gmail.com

[3)] *Department of Mathematics, Karunya Institute of Technology and Sciences*
Coimbatore-641114, Tamilnadu, India

[4)] *Department of Mechanical Engineering, Imam Khomieni International University*
Qazvin 34148-96818, Iran; e-mail: febrahimy@eng.ikiu.ac.ir

*Corresponding Author e-mail: selvamani@karunya.edu

In this paper, we study forced harmonic waves in a magneto-electro-viscoelastic (MEV) nanobeam embedded in a viscoelastic foundation using nonlocal strain gradient elasticity theory. The viscoelastic foundation is modeled as a Winkler-Pasternak layer. The governing equations of the nonlocal strain gradient viscoelastic nanobeam are derived using Hamilton's principle and solved analytically. A parametric study is presented to examine the effects of physical variables on the field. It is found that the effect of strain gradient and nonlocal parameter on dimensionless amplitude and phase angle is quite important. The findings from this study highlight the significance of identifying magneto-piezoelectricity in predicting the vibration characteristics of intelligent nanostructures and elucidating the impact of humid thermal effects on nanomaterials.

Keywords: piezoelectric nanobeam; vibration analysis; viscoelastic damping; nonlocal strain gradient; magneto-electro-viscoelastic.

1. Introduction

Magneto-electro-elastic (MEE) materials were first used in the 1970s. In 1974, Van Den Boomgard *et al.* [1] discovered MEE composites consisting of piezoelectric and piezomagnetic phases. MEE nanomaterials, including $BiFeO_3$,

$BiTiO_3$-$CoFe_2O_4$, $NiFe_2O_4$-PZT, and their nanostructures have played a significant role in research (ZHENG *et al.* [2], MARTIN *et al.* [3], WANG *et al.* [4], PRASHANTHI *et al.* [5]). For this reason, to harness the enormous potential of nanostructures and their applications, their mechanical behavior must be investigated and well identified before introducing new designs. Given these considerations, classical mechanic continuum theories are no longer suitable to predict the response of structures at very small scales, as they fail to provide accurate predictions. To address this problem, nonlocal theories (ERINGEN [6–11]) were presented which add a size parameter in the continuum modeling. Furthermore, various researchers (LI *et al.* [12], LAM *et al.* [13]) demonstrated that an increase in stiffness is not considered in nonlinear elasticity. Therefore, the nonlocal strain gradient theory was presented, where the stress field applies to not only the nonlocal stress field but also the strain gradients stress field. In this paper, the models that are developed according to Eringen's widely used nonlocal elasticity theory are studied.

Hence, PEDDIESON *et al.* [14] developed a nonlocal Euler-Bernoulli beam model by presenting a version of the nonlocal elasticity theory. The authors solved some representative problems, especially for cantilever beams to illustrate the magnitude of predicted nonlocal effects. ZENKOUR and SOBHY [15] studied the thermal buckling of single-layered graphene sheets on an elastic medium by using the sinusoidal shear deformation plate theory. Also, several researchers (WANG [16], WANG *et al.* [17], CIVALEK and DEMIR [18]) investigated the wave propagation and bending in carbon nanotubes (CNTs) and microtubules for nonlocal Euler-Bernoulli and Timoshenko beam models. In recent years, MURMU and PRADHAN [19] analyzed the small-size effects on single-walled carbon nanotubes (SWCNTs). They described the stability response of SWCNTs based on the nonlocal Timoshenko beam theory while considering an elastic medium. Additionally, the nonlocal parameter, the aspect ratio of the SWCNT, and Winkler and Pasternak parameters were studied.

YANG *et al.* [20] studied the nonlinear free vibration of SWCNTs based on Eringen's nonlocal elasticity theory and von Kármán geometric nonlinearity. They solved the obtained equations by using the differential quadrature (DQ) method. The free vibration, buckling and bending of Timoshenko nanobeams based on a meshless method were investigated by ROQUE *et al.* [21]. ŞIMŞEK and YURTCU [22] analyzed static bending and buckling of a functionally graded (FG) nanobeam under transvers distributed loads based on the nonlocal Timoshenko and Euler–Bernoulli beam theory. They derived the governing equations by applying the principal of the minimum total potential energy and solved analytically the resulting equations. A bending analysis of a thermo-magneto-electro-elastic nanobeam integrated with functionally graded piezomagnetic layers was conducted by AREFI and ZENKOUR [23]. SELVAMANI *et al.* [24] employed a nonlocal state-space strain gradient approach to study the vibration of piezoelectric functionally graded nanobeam. SELVAMANI *et al.* [25] discussed the static stability analysis of mass sensors consisting of hygro-thermally activated graphene sheets using a nonlocal strain gradient theory. The influence of rotation on a transversely isotropic piezoelectric rod coated with a thin film was reported by SELVAMANI and MAKINDE [26].

EBRAHIMI *et al.* [27] studied the thermal buckling analysis of magneto-electro-elastic (MEE) porous FG beam in a thermal environment. EBRAHIMI *et al.* [28] analyzed the bending behavior of magneto-electro-piezoelectric nanobeam system under hygro-thermal loading. KE *et al.* [29] investigated the free vibration of MEE nanoplates based on Eringen's nonlocal theory and Kirchhoff plate theory. In their analysis, the governing equations and boundary conditions for a MEE nanoplate subjected to biaxial force, external electric potential, external magnetic potential and temperature rise were derived using the Hamilton's principle and then solved analytically to obtain the natural frequencies of MEE nanoplates. They also studied the free vibration of the MEE nanobeam based on the Timoshenko beam theory and solved numerically the resulting equations. KE and WANG [30], however, did not investigate magneto-electro-viscoelastic nanobeams via nonlocal strain gradient theory in their research. A new tangential-exponential higher-order shear deformation theory for advanced composite plates was studied by MANTARI *et al.* [31].

EBRAHIMI and SALARI [32] analyzed the effect of various thermal loadings on the buckling and vibrational characteristics of nonlocal temperature-dependent FG nanobeams. EBRAHIMI *et al.* [33] investigated the dynamic characteristics of hygro-magneto-thermo-electrical nanobeam with non-ideal boundary conditions. EBRAHIMI *et al.* [34] reported the thermo-electro-elastic nonlinear stability analysis of viscoelastic double-piezo nanoplates under a magnetic field. SHEN *et al.* [35] investigated the modulation of topological structure including ultra-high energy density of graphene nanofiber. SAHMANI and AGHDAM [36] studied the nonlocal strain gradient beam model for nonlinear vibration in nanobeams.

To the best of the authors' knowledge, there has been no record regarding the nonlinear forced harmonic vibration of humid MEV nanobeam using the nonlocal strain gradient theory. Therefore, there is a strong scientific need to understand the nonlinear forced harmonic vibration of an MEV nanobeam in a humid thermal environment using the nonlocal strain gradient theory.

This paper investigates the forced harmonic vibration of a MEV nanobeam using the nonlocal strain gradient theory. Governing equations of a nanobeam resting on a viscoelastic substrate are derived based on Hamilton's principle. The multiple scale perturbation method is implemented to solve the governing equations. Effects of different factors, including shape parameter and nonlocal parameter, on damping vibration characteristics of a nanobeam are studied.

2. Theory and formulation multiscale composite

In Fig. 1, a piezoelectric nanobeam with length L, width b, and thickness h is illustrated.

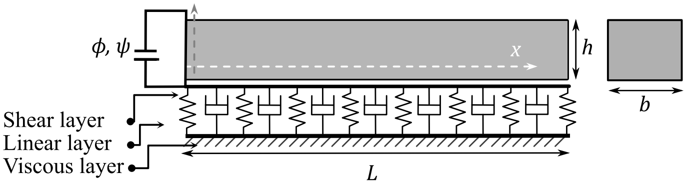

Fig. 1. Geometry of an MEV nanobeam resting on a viscoelastic foundation.

2.1. Multiscale model

The properties of the PCF shell, which is treated as orthotropic, can be presented as:

$$E_{11} = V_f E_{11}^F + V_{mcn}, \tag{2.1}$$

$$\frac{1}{E_{22}} = \frac{1}{E_{11}^F} + \frac{V_{mcn}}{E_{mcn}} - V_f V_{mnc} - \frac{\frac{V_f^2 E_{mcn}}{E_{22}^F} + \frac{V_{mcn}^2 E_{mcn}}{E^{mcn}} - 2V_f V_{mcn}}{V_f E_{22}^F + V_{mcn} E_{mcn}}, \tag{2.2}$$

$$\frac{1}{G_{12}} = \frac{V_f}{G_{11}^F} + \frac{V_{mcn}}{G_{mcn}}, \tag{2.3}$$

$$\rho = V_f \rho_f + V_{mcn} \rho_{mcn}, \tag{2.4}$$

$$\vartheta_{12} = V_f \upsilon_f + V_{mcn} \upsilon_{mcn}, \tag{2.5}$$

where E_{11}^F and E_{22}^F are Young's modulus of the CNT and G_{12} is the shear modulus ρ is the mass density, and ϑ_{12} represents Poisson's ratio of the fibers. The corresponding properties of the isotropic matrices in the CNT composite are E_{mcn}, G_{mcn}, ρ_{mcn} and V_{mcn} and the volume fractions of the fiber are represented by V_f.

Using the Halpin-Tsai model, composite tensile modulus is expressed as:

$$E_{mcn} = \frac{E_M}{8}\left[5\left(\frac{1 + 2\beta_{dd} V_{cn}}{1 - \beta_{dd} V_{cn}}\right) + 3\left(\frac{1 + 2(\frac{l_{cn}}{d_{cn}})\beta_{ll} V_{cn}}{1 - \beta_{ll} V_{cn}}\right)\right], \tag{2.6}$$

where

$$\beta_{ll} = \frac{\frac{E_{11}^{cn}}{E_M} - \frac{d_{ccn}}{4t^{cn}}}{\frac{E_{11}^{cn}}{E_M} + \frac{l_{cn}}{2h^{cn/gpl}}}, \tag{2.7}$$

$$\beta_{dd} = \frac{\frac{E_{11}^{cn}}{E_M} - \frac{d_{cn}}{4h^{cn}}}{\frac{E_{11}^{cn}}{E_M} + \frac{d_{cn}}{2h^{cn}}}, \tag{2.8}$$

where E_{11}^{cn} refers to Young's modulus, h^{cn}, d_{cn}, and l_{cn} represent thickness, outer diameter, and length, respectively, V_{cn} is the volume fraction of CNT, V_{mcn} and E_{mcn} are the volume fraction of the matrix and Young's modulus, respectively.

For the different distribution multiscale composite shells, we study how the weight fraction of CNT changes layer-wise in accordance with specific distribution patterns such as U, X, A, and O. The CNT volume fraction for the n-th layer corresponding to each distribution pattern can be expressed as:

$$\begin{aligned} &U\colon\ V_{cn}^{n} = V_{cn}, \\ &X\colon\ V_{cn}^{n} = 2V_{cn}\left(\frac{|2n - n_t - 1|}{n_t}\right), \\ &O\colon\ V_{cn}^{n} = 2V_{cn}\left(1 - \frac{|2n - n_t - 1|}{n_t}\right), \\ &A\colon\ V_{cn}^{n} = V_{cn}\left(\frac{|2n - 1|}{n_t}\right), \end{aligned} \tag{2.9}$$

where the total number of layers is expressed by n_t and the total volume fraction of CNT can be determined by:

$$V_{cn} = \frac{w_{cn}}{w_{cn} + \left(\frac{\rho_{cn}}{\rho_m}\right) - \left(\frac{\rho_{cn}}{\rho_m}\right) w_{cn}}, \tag{2.10}$$

where ρ_{cn} are the mass densities of the CNT, ρ_m is the mass density of the epoxy resin matrix, and $w_{cn}$is the mass fraction of the CNT.

The relationships between mass density, modulus, and Poisson's ratio for the CNT can be expressed as follows:

$$\rho_{mnc} = V_{cn}\rho_{cn} + v_m\rho_m, \tag{2.11}$$

$$G_{mnc} = \frac{E_{mnc}}{2(1 + v_{mcn})}, \tag{2.12}$$

$$V_{mcn} = V_m, \tag{2.13}$$

where v_m and v_{mcn} are Poisson's ratio of the matrix and CNT and α_{11} refers to the thermal expansion coefficients in the longitudinal direction and α_{22} in the transverse direction.

The thermal expansion coefficients of the longitudinal and transverse directions of the fiber α_{11}^{f} and α_{22}^{f}, and the thermal expansion of the CNT α_{mcn} can be expressed as [12]:

$$\alpha_{11} = \frac{V_f E_{11}^{f} \alpha_{11}^{f} + V_{mcn} E_{mcn} \alpha_{mcn}}{V_f E_{11}^{f} + V_{mcn} E_{mcn}}, \tag{2.14}$$

$$\alpha_{22} = (1 + V_f)\, V_f \alpha_{22}^{f} + (1 + V_{mnc})\, V_{mcn} \alpha_{mcn} - v_{12}\alpha_{11}, \tag{2.15}$$

$$\alpha_{mcn} = \frac{1}{2}\left(\frac{V_{cn} E_{cn} \alpha_{cn} + v_m E_m \alpha_m}{v_{cn} E_{cn} + v_m E_m}\right)(1 - v_{mcn}) + (1 + v_m)\alpha_m V_m + (1 + v_{cn})\alpha_{cn} V_{cn}, \tag{2.16}$$

where α_{mcn}, β_{mcn} are the thermal expansion and moisture coefficients of the epoxy resin CNT matrix and α_{cn} is the thermal expansion coefficient of the CNT.

$$\beta_{11} = \frac{V_f E_{11}^{f} + V_{mcn} E_{mcn} \beta_m}{V_f E_{11}^{f} + V_{mcn} E_{mcn}}, \tag{2.17}$$

$$\beta_{22} = (1 + V_{mcn})\, V_{mcn} \beta_m - v_{12}\beta_{11}. \tag{2.18}$$

If we define α_{mcn}, β_{mcn} and its parameters are hypothetical.

2.2. Kinematic relations

The displacement field of the refined shear deformable nanobeam can be expressed as:

$$\overline{u}(x, z, t) = u(x, t) - z\frac{\partial w_b}{\partial x} - f(z)\frac{\partial w_s}{\partial x}, \tag{2.19}$$

$$\overline{w}(x, z, t) = w_b(x, t) + w_s(x, t), \tag{2.20}$$

where u is the axial mid-plane displacement, and w_b, w_s denote the bending and shear components of transverse displacement, respectively. Also, $f(z)$ is the shape function representing the shear stress/strain distribution through the beam thickness. For the present study has a trigonometric nature, and thus, a shear correction factor is not required (Mantari *et al.* [31]):

$$f(z) = z - \tan(mz), \qquad m = 0.03. \tag{2.21}$$

The non-zero strains of the suggested beam model can be expressed as follows:

$$\varepsilon_{xx} = \frac{\partial u}{\partial x} - z\frac{\partial^2 w_b}{\partial x^2} - f(z)\frac{\partial^2 w_s}{\partial x^2}, \tag{2.22}$$

$$\gamma_{xz} = g(z)\frac{\partial w_s}{\partial x}, \tag{2.23}$$

where $g(z) = 1 - \mathrm{d}f(z)/\mathrm{d}z$. According to Maxwell's equation, the electric potential $\varPhi$ and magnetic potential $\varPsi$ distributions across the thickness of the nanobeam are approximated as follows [30]:

$$\varPhi(x,z,t) = -\cos(\beta z)\phi(x,t) + \frac{2z}{h}V, \tag{2.24}$$

$$\varPsi(x,z,t) = -\cos(\beta z)\psi(x,t) + \frac{2z}{h}\varOmega, \tag{2.25}$$

in which $\beta = \pi/h$. Also, V and $\varOmega$ are the external electric voltage and magnetic potential applied to the nanobeam, respectively. The relationship between electric field (E_x, E_z) and electric potential (ϕ) and also magnetic field (H_x, H_z) and magnetic potential (ψ), can be obtained as:

$$E_x = -\varPhi_{,x} = \cos(\beta z)\frac{\partial \phi}{\partial x}, \tag{2.26}$$

$$E_z = -\varPhi_{,z} = -\beta\sin(\beta z)\phi(x,t) - \frac{2V}{h}, \tag{2.27}$$

$$H_x = -\varPsi_{,x} = \cos(\beta z)\frac{\partial \psi}{\partial x}, \tag{2.28}$$

$$H_z = -\varPsi_{,z} = -\beta\sin(\beta z)\psi(x,t) - \frac{2\varOmega}{h}. \tag{2.29}$$

Through an extended Hamilton's principle, the governing equations can be derived as follows:

$$\int_0^t \delta(\varPi_S - \varPi_K + \varPi_W)\,\mathrm{d}t = 0, \tag{2.30}$$

where $\varPi_S$ is the total strain energy, $\varPi_K$ is the kinetic energy, and $\varPi_W$ is the work done by external applied forces. The strain energy $\varPi_S$ can be calculated as:

$$\varPi_S = \frac{1}{2}\int_V (\sigma_{xx}\varepsilon_{xx} + \sigma_{xz}\gamma_{xz} - D_x E_x - D_z E_z - B_x H_x - B_z H_z)\,\mathrm{d}V. \tag{2.31}$$

By calculating the first variation of strain energy Π_S and substituting Eqs. (2.22)–(2.23) into Eq. (2.31) yields:

$$\delta\Pi_S = \int_0^L \left(N\frac{\partial\delta u}{\partial x} - M_b\frac{\partial^2\delta w_b}{\partial x^2} - M_s\frac{\partial^2\delta w_s}{\partial x^2} + Q\frac{\partial\delta w_s}{\partial x} \right)\mathrm{d}x + \int_0^L \left(-\overline{D}_x\frac{\partial\delta\phi}{\partial x} + \overline{D}_z\delta\phi - \overline{B}_x\frac{\partial\delta\psi}{\partial x} + \overline{B}_z\delta\psi \right)\mathrm{d}x. \tag{2.32}$$

The variables expressed in the above equation are defined as follows:

$$(N, M_b, M_s) = \int_{-h/2}^{h/2} \sigma_{xx}(1, z, f(z))\,\mathrm{d}z, \tag{2.33}$$

$$Q = \int_{-h/2}^{h/2} \sigma_{xz}g(z)\,\mathrm{d}z, \tag{2.34}$$

$$(\overline{D}_x, \overline{B}_x) = \int_{-h/2}^{h/2} (D_x, B_x)\cos(\beta z)\,\mathrm{d}z, \tag{2.35}$$

$$(\overline{D}_z, \overline{B}_z) = \int_{-h/2}^{h/2} (D_z, B_z)\xi\sin(\beta z)\,\mathrm{d}z, \tag{2.36}$$

where σ_{ij}, ε_{ij}, D_i, B_i, E_i, H_i, N, M_i, and Q are the stress, strain, electric displacement, magnetic induction electric field, magnetic field, the axial force, bending moment and shear force resultants, respectively. The kinetic energy can be expressed as follows:

$$\Pi_K = \frac{1}{2}\int_V \rho\left[\left(\frac{\partial\overline{u}}{\partial t}\right)^2 + \left(\frac{\partial\overline{w}}{\partial t}\right)^2\right]\mathrm{d}V. \tag{2.37}$$

Also, the first variation of kinetic energy of present theory can be written in the form:

$$\delta \Pi_K = \int_0^L \left[I_0 \left(\frac{\partial u}{\partial t}\frac{\partial \delta u}{\partial t} + \frac{\partial (w_b + w_s)}{\partial t}\frac{\partial \delta (w_b + w_s)}{\partial t} \right) \right. \tag{2.38}$$

$$- I_1 \left(\frac{\partial u}{\partial t}\frac{\partial^2 w_b}{\partial t \partial x} + \frac{\partial^2 w_b}{\partial t \partial x}\frac{\partial \delta u}{\partial t} \right) - I_2 \left(\frac{\partial u}{\partial t}\frac{\partial^2 \delta w_s}{\partial t \partial x} + \frac{\partial^2 w_s}{\partial t \partial x}\frac{\partial \delta u}{\partial t} \right)$$

$$\left. + I_3 \left(\frac{\partial^2 w_b}{\partial t \partial x}\frac{\partial^2 \delta w_s}{\partial t \partial x} + \frac{\partial^2 w_s}{\partial t \partial x}\frac{\partial^2 \delta w_b}{\partial t \partial x} \right) + I_4 \frac{\partial^2 w_b}{\partial t \partial x}\frac{\partial^2 \delta w_b}{\partial t \partial x} + I_5 \frac{\partial^2 w_s}{\partial t \partial x}\frac{\partial^2 \delta w_s}{\partial t \partial x} \right] \mathrm{d}x,$$

in which the mass inertia are defined as:

$$(I_0, I_1, I_2, I_3, I_4, I_5) = \int_{-h/2}^{h/2} \rho \left(1, z, f(z), z f(z), z^2, f^2(z)\right) \mathrm{d}z. \tag{2.39}$$

The work done by applied forces and its first variation are expressed by:

$$\Pi_W = \int_0^L \left[F\left(w_b + w_s\right) - \frac{1}{2}\left(N^E + N^H\right)\left(\frac{\partial \left(w_b + w_s\right)}{\partial x}\right)^2 \right] \mathrm{d}x, \tag{2.40}$$

$$\delta \Pi_w = \int_0^L \left[F \delta \left(w_b + w_s\right) - \left(N^E + N^H\right) \frac{\partial \left(w_b + w_s\right)}{\partial x}\frac{\partial \delta \left(w_b + w_s\right)}{\partial x} \right] \mathrm{d}x, \tag{2.41}$$

in which F denotes the external transverse load from the viscoelastic medium which is obtained as:

$$F = k_w \left(w_b + w_s\right) - k_p \frac{\partial^2 \left(w_b + w_s\right)}{\partial x^2} + c_d \frac{\partial \left(w_b + w_s\right)}{\partial t}, \tag{2.42}$$

where k_w, k_p, and c_d are the linear, shear and damping coefficients of the medium. Also, N^E and N^H denote electric and magnetic loading, respectively.

The following Euler-Lagrange equations are obtained by inserting Eqs. (2.32), (2.38), and (2.41) into Eq. (2.40) and integrating by parts, with the coefficients of δu, δw_b, δw_s, $\delta \phi$, $\delta \psi$ equal to zero, resulting in the following set of equations:

$$\frac{\partial N}{\partial x} = I_0 \frac{\partial^2 u}{\partial t^2} - I_1 \frac{\partial^3 w_b}{\partial x \partial t^2} - I_2 \frac{\partial^3 w_s}{\partial x \partial t^2}, \tag{2.43}$$

$$\frac{\partial^2 M_b}{\partial x^2} = I_0 \frac{\partial^2 \left(w_b + w_s\right)}{\partial t^2} + I_1 \frac{\partial^3 u}{\partial x \partial t^2} - I_3 \frac{\partial^4 w_s}{\partial x^2 \partial t^2} \tag{2.44}$$

$$- I_4 \frac{\partial^4 w_b}{\partial x^2 \partial t^2} + \left(N^E + N^B\right) \frac{\partial^2 \left(w_b + w_s\right)}{\partial x^2} + F,$$

$$\frac{\partial^2 M_s}{\partial x^2} + \frac{\partial Q}{\partial x} = I_0 \frac{\partial^2 (w_b + w_s)}{\partial t^2} + I_2 \frac{\partial^3 u}{\partial t^2 \partial x} - I_3 \frac{\partial^4 w_b}{\partial t^2 \partial x^2} - I_5 \frac{\partial^4 w_s}{\partial t^2 \partial x^2} + \left(N^E + N^B\right) \frac{\partial^2 (w_b + w_s)}{\partial x^2} + F, \tag{2.45}$$

$$\frac{\partial \overline{D}_x}{\partial x} + \overline{D}_z = 0, \tag{2.46}$$

$$\frac{\partial \overline{B}_x}{\partial x} + \overline{B}_z = 0. \tag{2.47}$$

2.3. The nonlocal strain gradient theory for MEV materials

In Eringen's nonlocal theory of elasticity, the stress state at a reference point $\mathbf{x}$ in an elastic continuum is not only dependent on the strain state at $\mathbf{x}$ but also on the strain state at all other points $\mathbf{x}'$ in the body. In addition, based on the nonlocal strain gradient theory developed by LAM *et al.* [13], the stress accounts for both the nonlocal elastic stress field and the strain gradient stress field. Therefore, the stress can be expressed as follows:

$$\sigma_{ij} = \sigma_{ij}^{(0)} - \nabla \sigma_{ij}^{(1)}, \tag{2.48}$$

where the stress $\sigma_{ij}^{(0)}$ corresponds to strain ε_{ij} and the higher-order stress $\sigma_{ij}^{(1)}$ corresponds to the strain gradient $\nabla \varepsilon_{ij}$. They are defined as:

$$\sigma_{ij}^{(0)} = \int_0^L \alpha_0 \left(\mathbf{x}, \mathbf{x}', e_0 a/l\right) \sigma_{ij}^c \left(\mathbf{x}'\right) \mathrm{d}\mathbf{x}', \tag{2.49}$$

$$\sigma_{ij}^{(1)} = l^2 \int_0^L \alpha_1 \left(\mathbf{x}, \mathbf{x}', e_1 a/l\right) \nabla \sigma_{ij}^c \left(\mathbf{x}'\right) \mathrm{d}\mathbf{x}', \tag{2.50}$$

where L is the length of the nanobeam, σ_{ij}^c is the classical stress components at any point $\mathbf{x}'$ in the body, $\alpha_i \left(\mathbf{x}, \mathbf{x}', e_i a/l\right)$ is the kernel of the integral equation, in which a and l correspond to the nonlocalness and denote the internal characteristic length (lattice parameter, size of grain, or granular distance) and the external characteristic length of the system (wavelength, crack length, size, or dimensions of the sample), respectively, and e_i is a constant appropriate to the material and has to be determined independently for each material. When the nonlocal functions $\alpha_i \left(\mathbf{x}, \mathbf{x}', e_i a/l\right)$ satisfy the conditions developed by ERINGEN [11], the linear nonlocal differential operator can be assumed as follows:

$$\mathbb{L}_i = 1 - \left(e_i a\right)^2 \nabla^2 \quad \text{for} \quad i = 0, 1. \tag{2.51}$$

By applying Eq. (2.33) into Eq. (2.30), a general constitutive relation in a differential form for a nanobeam can be stated as:

$$\left[1-(e_1a)^2\nabla^2\right]\left[1-(e_0a)^2\nabla^2\right]\sigma_{ij}=\left[1-(e_1a)^2\nabla^2\right]\sigma_{ij}^c - \left[1-(e_0a)^2\nabla^2\right]l^2\nabla^2\sigma_{ij}^c, \tag{2.52}$$

where $\nabla^2=\partial^2/\partial x^2$ denotes the Laplacian operator. By retaining terms of order $o(\nabla^2)$ and assuming $e_0=e_1=e$, the general constitutive relation in a simplified form can be written as follows:

$$\left[1-(ea)^2\nabla^2\right]\sigma_{ij}=\left(1-l^2\nabla^2\right)\sigma_{ij}^c. \tag{2.53}$$

Similarly, the following equations are obtained for a MEV nanobeam:

$$\left[1-(ea)^2\nabla^2\right]D_j=\left(1-l^2\nabla^2\right)D_j^c, \tag{2.54}$$

$$\left[1-(ea)^2\nabla^2\right]B_j=\left(1-l^2\nabla^2\right)B_j^c. \tag{2.55}$$

In the above equations, σ_{ij}^c, D_j^c and B_j^c are given by Ke *et al.* [29] as follows:

$$\sigma_{ij}^c=C_{ijkl}\varepsilon_{kl}-e_{mij}E_m-q_{nij}H_n, \tag{2.56}$$

$$D_j^c=e_{jkl}\varepsilon_{kl}+\chi_{jm}E_m+d_{jn}H_n, \tag{2.57}$$

$$B_j^c=q_{jkl}\varepsilon_{kl}+d_{jm}E_m+\lambda_{jn}H_n, \tag{2.58}$$

where ε_{kl} is the strain and C_{ijkl}, e_{mij}, χ_{jm}, q_{nij}, d_{jn}, and λ_{jn} denote the elastic, piezoelectric, dielectric, piezomagnetic, magnetoelectric and magnetic constants, respectively. Finally, the stress-strain relations of a MEV solid can be expressed as:

$$\left[1-\mu\nabla^2\right]\sigma_{xx}=\left(1-\lambda\nabla^2\right)[C_{11}\varepsilon_{xx}-e_{31}E_z-q_{31}H_z], \tag{2.59}$$

$$\left[1-\mu\nabla^2\right]\sigma_{xz}=\left(1-\lambda\nabla^2\right)[C_{55}\gamma_{xz}-e_{15}E_x-q_{15}H_x], \tag{2.60}$$

$$\left[1-\mu\nabla^2\right]D_x=\left(1-\lambda\nabla^2\right)[e_{15}\gamma_{xz}+\chi_{11}E_x+d_{11}H_x], \tag{2.61}$$

$$\left[1-\mu\nabla^2\right]D_z=\left(1-\lambda\nabla^2\right)[e_{31}\varepsilon_{xx}+\chi_{33}E_z+d_{33}H_z], \tag{2.62}$$

$$\left[1-\mu\nabla^2\right]B_x=\left(1-\lambda\nabla^2\right)[q_{15}\gamma_{xz}+d_{11}E_x+\lambda_{11}H_x], \tag{2.63}$$

$$\left[1-\mu\nabla^2\right]B_z=\left(1-\lambda\nabla^2\right)[q_{31}\varepsilon_{xx}+d_{33}E_z+\lambda_{33}H_z], \tag{2.64}$$

where $\mu=(ea)^2$ and $\lambda=l^2$.

Applying the Kelvin-Voigt viscoelastic damping model with the damping coefficient (g_0) and integrating Eq. (2.59)–(2.64) over the cross-section area of the nanobeam provides the following nonlocal relations for a refined beam model:

$$N-\mu\frac{\partial^2 N}{\partial x^2}=(1-\beta\nabla^2)\left[\left(1+g_0\frac{\partial}{\partial t}\right)\left(J_{11}\frac{\partial u}{\partial x}-J_{11}^{z}\frac{\partial^2 w_b}{\partial x^2}-J_{11}^{f}\frac{\partial^2 w_s}{\partial x^2}\right)+K_{31}^{e}\phi+K_{31}^{m}\psi-N^{E}-N^{H}\right],\tag{2.65}$$

$$M_b-\mu\frac{\partial^2 M_b}{\partial x^2}=(1-\beta\nabla^2)\left[\left(1+g_0\frac{\partial}{\partial t}\right)\left(J_{11}^{z}\frac{\partial u}{\partial x}-J_{11}^{zz}\frac{\partial^2 w_b}{\partial x^2}-J_{11}^{zf}\frac{\partial^2 w_s}{\partial x^2}\right)+X_{31}^{e}\phi+X_{31}^{m}\psi-M_b^{E}-M_b^{H}\right],\tag{2.66}$$

$$M_s-\mu\frac{\partial^2 M_s}{\partial x^2}=(1-\beta\nabla^2)\left[\left(1+g_0\frac{\partial}{\partial t}\right)\left(J_{11}^{f}\frac{\partial u}{\partial x}-J_{11}^{zf}\frac{\partial^2 w_b}{\partial x^2}-J_{11}^{ff}\frac{\partial^2 w_s}{\partial x^2}\right)+Y_{31}^{e}\phi+Y_{31}^{m}\psi-M_s^{E}-M_s^{H}\right],\tag{2.67}$$

$$Q-\mu\frac{\partial^2 Q}{\partial x^2}=(1-\beta\nabla^2)\left[\left(1+g_0\frac{\partial}{\partial t}\right)\left(K_{55}\frac{\partial w_s}{\partial x}\right)-X_{15}\frac{\partial\phi}{\partial x}-Y_{15}\frac{\partial\psi}{\partial x}\right],\tag{2.68}$$

$$\overline{D}_x-\mu\frac{\partial^2 d_x}{\partial x^2}=(1-\beta\nabla^2)\left(X_{15}\frac{\partial w_s}{\partial x}+X_{11}\frac{\partial\phi}{\partial x}+Y_{11}\frac{\partial\psi}{\partial x}\right),\tag{2.69}$$

$$\overline{D}_z-\mu\frac{\partial^2 d_z}{\partial x^2}=(1-\beta\nabla^2)\left(K_{31}^{e}\frac{\partial u}{\partial x}-X_{31}^{e}\frac{\partial^2 w_b}{\partial x^2}-Y_{31}^{e}\frac{\partial^2 w_s}{\partial x^2}-X_{33}\phi-Y_{33}\psi-F_{33}^{e}\right),\tag{2.70}$$

$$\overline{B}_x-\mu\frac{\partial^2 b_x}{\partial x^2}=(1-\beta\nabla^2)\left(Y_{15}\frac{\partial w_s}{\partial x}+Y_{11}\frac{\partial\phi}{\partial x}+K_{11}\frac{\partial\psi}{\partial x}\right),\tag{2.71}$$

$$\overline{B}_z-\mu\frac{\partial^2 b_z}{\partial x^2}=(1-\beta\nabla^2)\left(K_{31}^{m}\frac{\partial u}{\partial x}-X_{31}^{m}\frac{\partial^2 w_b}{\partial x^2}-Y_{31}^{m}\frac{\partial^2 w_s}{\partial x^2}-Y_{33}\phi-K_{33}\psi-F_{33}^{m}\right).\tag{2.72}$$

In the above equations, the cross-sectional rigidities are expressed as follows:

$$\left(J_{11}, J_{11}^{z}, J_{11}^{f}, J_{11}^{zz}, J_{11}^{zf}, J_{11}^{ff}\right) = \int_{-h/2}^{h/2} C_{11}\left(1, z, f, z^2, zf, f^2\right) \mathrm{d}z, \tag{2.73}$$

$$\left(K_{31}^{e}, X_{31}^{e}, Y_{31}^{e}\right) = \int_{-h/2}^{h/2} e_{31}\gamma \sin(\gamma z)\,(1, z, f)\,\mathrm{d}z, \tag{2.74}$$

$$\left(K_{31}^{m}, X_{31}^{m}, Y_{31}^{m}\right) = \int_{-h/2}^{h/2} q_{31}\gamma \sin(\gamma z)\,(1, z, f)\,\mathrm{d}z, \tag{2.75}$$

$$K_{55} = \int_{-h/2}^{h/2} C_{55}\, g^2(z)\,\mathrm{d}z, \tag{2.76}$$

$$\left(X_{15}, Y_{15}\right) = \int_{-h/2}^{h/2} \left(e_{15}, q_{15}\right) g \cos(\gamma z)\,\mathrm{d}z, \tag{2.77}$$

$$\left(X_{11}, Y_{11}, K_{11}\right) = \int_{-h/2}^{h/2} \left(\chi_{11}, d_{11}, \lambda_{11}\right) \cos^2(\gamma z)\,\mathrm{d}z, \tag{2.78}$$

$$\left(X_{33}, Y_{33}, K_{33}\right) = \int_{-h/2}^{h/2} \left(\chi_{33}, d_{33}, \lambda_{33}\right)\beta^2 \sin^2(\gamma z)\,\mathrm{d}z, \tag{2.79}$$

$$\left(F_{33}^{e}, F_{33}^{m}\right) = \int_{-h/2}^{h/2} \left(\chi_{33}\frac{2V}{h} + d_{33}\frac{2\Omega}{h},\; d_{33}\frac{2V}{h} + \lambda_{33}\frac{2\Omega}{h}\right) \gamma \sin(\gamma z)\,\mathrm{d}z. \tag{2.80}$$

Also, the summation of normal forces and moments due to magneto-electrical field can be defined as:

$$\left(N^{E} + N^{H}, M_b^{E} + M_b^{H}, M_s^{E} + M_s^{H}\right) = -\int_{-h/2}^{h/2} \left(e_{31}\frac{2V}{h} + q_{31}\frac{2\Omega}{h}\right)(1, z, f)\,\mathrm{d}z. \tag{2.81}$$

The governing equations of a refined nanobeam under electrical and magnetic fields based on the nonlocal strain gradient theory in terms of the displacement can be obtained by substituting Eqs. (2.55)–(2.54) into Eqs. (2.33)–(2.37) as follows:

$$\begin{aligned}(2.82)\quad &\left(1-\mu\nabla^2\right)\left(I_0\frac{\partial^2 u}{\partial t^2}-I_1\frac{\partial^3 w_b}{\partial t^2\partial x}-I_2\frac{\partial^3 w_s}{\partial t^2\partial x}\right)-\left(1-\beta\nabla^2\right)\\&\cdot\left[\left(1+g_0\frac{\partial}{\partial t}\right)\left(J_{11}\frac{\partial^2 u}{\partial x^2}-J_{11}^{z}\frac{\partial^3 w_b}{\partial x^3}-J_{11}^{f}\frac{\partial^3 w_s}{\partial x^3}\right)+K_{31}^{e}\frac{\partial\phi}{\partial x}+K_{31}^{m}\frac{\partial\psi}{\partial x}\right]=0,\end{aligned}$$

$$\begin{aligned}(2.83)\quad &\left(1-\mu\nabla^2\right)\Bigg(I_0\frac{\partial^2\left(w_b+w_s\right)}{\partial t^2}+I_1\frac{\partial^3 u}{\partial t^2\partial x}-I_3\frac{\partial^4 w_s}{\partial t^2\partial x^2}\\&-I_4\frac{\partial^4 w_b}{\partial t^2\partial x^2}+\left(N^E+N^H\right)\frac{\partial^2\left(w_b+w_s\right)}{\partial x^2}\\&+k_w\left(w_b+w_s\right)-k_p\frac{\partial^2\left(w_b+w_s\right)}{\partial x^2}+c_d\frac{\partial\left(w_b+w_s\right)}{\partial t}\Bigg)\\&-\left(1-\beta\nabla^2\right)\Bigg[\left(1+g_0\frac{\partial}{\partial t}\right)\left(J_{11}^{z}\frac{\partial^3 u}{\partial x^3}-J_{11}^{zz}\frac{\partial^4 w_b}{\partial x^4}-J_{11}^{zf}\frac{\partial^4 w_s}{\partial x^4}\right)\\&+X_{31}^{e}\frac{\partial^2\phi}{\partial x^2}+X_{31}^{m}\frac{\partial^2\psi}{\partial x^2}\Bigg]=0,\end{aligned}$$

$$\begin{aligned}(2.84)\quad &\left(1-\mu\nabla^2\right)\Bigg(I_0\frac{\partial^2\left(w_b+w_s\right)}{\partial t^2}+I_2\frac{\partial^3 u}{\partial t^2\partial x}-I_3\frac{\partial^4 w_b}{\partial t^2\partial x^2}\\&-I_5\frac{\partial^4 w_s}{\partial t^2\partial x^2}+\left(N^E+N^H\right)\frac{\partial^2\left(w_b+w_s\right)}{\partial x^2}\\&+k_w\left(w_b+w_s\right)-k_p\frac{\partial^2\left(w_b+w_s\right)}{\partial x^2}+c_d\frac{\partial\left(w_b+w_s\right)}{\partial t}\Bigg)\\&-\left(1-\lambda\nabla^2\right)\Bigg[\left(1+g_0\frac{\partial}{\partial t}\right)\left(J_{11}^{f}\frac{\partial^3 u}{\partial x^3}-J_{11}^{zf}\frac{\partial^4 w_b}{\partial x^4}-J_{11}^{ff}\frac{\partial^4 w_s}{\partial x^4}+K_{55}\frac{\partial^2 w_s}{\partial x^2}\right)\\&+\left(Y_{31}^{e}-X_{15}\right)\frac{\partial^2\phi}{\partial x^2}+\left(Y_{31}^{m}-Y_{15}\right)\frac{\partial^2\psi}{\partial x^2}\Bigg]=0,\end{aligned}$$

$$\begin{aligned}(2.85)\quad &\left(1-\lambda\nabla^2\right)\Bigg(K_{31}^{e}\frac{\partial u}{\partial x}-X_{31}^{e}\frac{\partial^2 w_b}{\partial x^2}+\left(X_{15}-Y_{31}^{e}\right)\frac{\partial^2 w_s}{\partial x^2}\\&+X_{11}\frac{\partial^2\phi}{\partial x^2}+Y_{11}\frac{\partial^2\psi}{\partial x^2}-X_{33}\phi-Y_{33}\psi-F_{33}^{e}\Bigg)=0,\end{aligned}$$

$$(1-\lambda\nabla^2)\left(K_{31}^m\frac{\partial u}{\partial x}-X_{31}^m\frac{\partial^2 w_b}{\partial x^2}+(Y_{15}-Y_{31}^m)\frac{\partial^2 w_s}{\partial x^2}\right.$$
$$\left.+Y_{11}\frac{\partial^2\phi}{\partial x^2}+K_{11}\frac{\partial^2\psi}{\partial x^2}-Y_{33}\phi-K_{33}\psi-F_{33}^m\right)=0 \tag{2.86}$$

(see Appendix).

3. Solution procedure

The following boundary conditions for an exact solution of the governing equations of a magneto-electro-viscoelastic nanobeam are expressed as:

- simply-supported (S):

$$w_b=w_s=M=\frac{\partial u}{\partial x}=0 \qquad \text{at} \qquad x=0,L. \tag{3.1}$$

- clamped (C):

$$u=w_b=w_s=\frac{\partial(w_b+w_s)}{\partial x}=0 \qquad \text{at} \qquad x=0,L. \tag{3.2}$$

According to the above boundary conditions, the displacement quantities are presented in Eq. (3.3)–(3.7) as:

$$u(x,t)=\sum_{n=1}^{\infty}U_n\frac{\partial X_n(x)}{\partial x}e^{i\omega_n t}, \tag{3.3}$$

$$w_b(x,t)=\sum_{n=1}^{\infty}W_{bn}X_n(x)e^{i\omega_n t}, \tag{3.4}$$

$$w_s(x,t)=\sum_{n=1}^{\infty}W_{sn}X_n(x)e^{i\omega_n t}, \tag{3.5}$$

$$\phi(x,t)=\sum_{n=1}^{\infty}\Phi_n X_n(x)e^{i\omega_n t}, \tag{3.6}$$

$$\psi(x,t)=\sum_{n=1}^{\infty}\Psi_n X_n(x)e^{i\omega_n t}. \tag{3.7}$$

The admissible function X_n is considered as a mode shape according to boundary conditions as follows [33]:

$$\text{S–S}: \ X_n = \sin\left(\frac{n\pi}{L}x\right), \tag{3.8}$$

$$\text{C–C}: \ X_n = \sin^2\left(\frac{n\pi}{L}x\right). \tag{3.9}$$

Finally, Eqs. (2.4)–(2.7) can be written as:

$$EI\frac{\partial^4\hat{w}}{\partial\widehat{x}^4} + m\frac{\partial^2\widehat{w}}{\partial\widehat{t}^2} + \widehat{P}\frac{\partial^2\widehat{w}}{\partial\widehat{x}^2} + \widehat{C}\frac{\partial\widehat{w}}{\partial\widehat{t}} - \frac{EA}{2L}\frac{\partial^2\widehat{w}}{\partial\widehat{x}^2}\int_0^L\left(\frac{\partial\widehat{w}}{\partial\widehat{x}}\right)^2 \mathrm{d}\widehat{x} = \widehat{F}\left(\widehat{x}\right)\cos\left(\widehat{\Omega}\,\widehat{t}\right). \tag{3.10}$$

3.1. *Primary resonance*

In the primary resonance case, it is assumed that the excitation frequency and the linear frequency of the system ω_0 are close to each other and therefore $\Omega = \omega_0$. So a detuning parameter σ is employed to illustrate how close Ω is to ω_0:

$$\omega^2 = \Omega + \varepsilon\sigma, \tag{3.11}$$

where σ is the detuning parameter.

The uniformly approximate solutions of Eq. (3.10) are obtained as:

$$w = w_0\left(T_0, T_1, T_2, ...\right) + \varepsilon w_1\left(T_0, T_1, T_2, ...\right) + \varepsilon^2 w_2\left(T_0, T_1, T_2, ...\right), \tag{3.12}$$

where $T_0 = t$ and $T_1 = \varepsilon t$.

The terms of T_0 and T_1 are expressed as:

$$F(t) = \varepsilon\overline{q}\cos\left(\omega_0 T_0 + \sigma T_1\right), \tag{3.13}$$

the derivatives to t yield:

$$\frac{\mathrm{d}}{\mathrm{d}t} = D_0 + \varepsilon D_1, \tag{3.14}$$

$$\frac{\mathrm{d}}{\mathrm{d}t} = D_0^2 + 2\varepsilon D_0 D_1 + \varepsilon^2(D_1^2 + 2D_0 D_1). \tag{3.15}$$

Substituting Eqs. (3.14) and (3.15) and equating the coefficients of ε to zero yield the following differential equations:

$$\varepsilon^0 : D_0^2 w_0 + \Omega^2 w_0 = 0, \tag{3.16}$$

$$\varepsilon^1 : D_0^2 w_1 + \Omega^2 w_1 = -2D_0 D_1 w_0 - \mu D_0 w_0 - P_3 w_0^3 - k\cos(\omega_0 T_0 + \sigma T_1). \tag{3.17}$$

With this approach, it is convenient to write the solution of Eq. (3.12) as:

$$w_0(T_0, T_1, T_2, \ldots) = \exp(iT_0) + \overline{A}\exp(-iT_0), \tag{3.18}$$

where A is an unknown complex function and $\overline{A}$ is the complex conjugate of A. By requiring w_1 to be periodic in T_0 and extracting the secular terms that are coefficients of $e^{\pm i\omega_0 T_0}$ the governing equation is determined as:

$$2i\omega_0(A' + \mu A) + 3P_3 A^2\,\overline{A} - \frac{1}{2}k\exp(-i\sigma T_1) = 0. \tag{3.19}$$

Assuming that A is in polar form:

$$A = \frac{1}{2}a\exp(i\gamma), \tag{3.20}$$

where a and γ are real parameters. Separating these term parts of the derived equation results in:

$$a' = -\mu a + \frac{1}{2}\frac{\overline{q}}{\omega_0}\sin(\sigma T_1 - \gamma), \tag{3.21}$$

$$a\gamma' = \frac{3}{8}\frac{P_3}{\omega_0}a^3 - \frac{1}{2}\frac{\overline{q}}{\omega_0}\cos(\sigma T_1 - \gamma). \tag{3.22}$$

Now, by introducing

$$\theta = \sigma T_1 - \gamma, \tag{3.23}$$

and substituting Eq. (3.23) into Eqs. (3.21) and (3.22) yield:

$$a' = -\mu a + \frac{1}{2}\frac{\overline{q}}{\omega_0}\sin\theta, \tag{3.24}$$

$$a\gamma' = \frac{3}{8}\frac{P_3}{\omega_0}a^3 - \frac{1}{2}\frac{\overline{q}}{\omega_0}\cos\theta. \tag{3.25}$$

The singular point of this system at $a' = 0$ and $\theta' = 0$ represents the steady-state motion of the system. So, in the steady-state condition, the system can be expressed as:

$$a = -\mu a + \frac{1}{2}\frac{\bar{q}}{\omega_0}\sin\theta, \tag{3.26}$$

$$\sigma a - \frac{3}{8}\frac{P_3}{\omega_0}a^3 = -\frac{1}{2}\frac{\bar{q}}{\omega_0}\cos\theta. \tag{3.27}$$

The fixed points of Eqs. (3.26) and (3.27) correspond to solutions with constant amplitude and phase. These solutions satisfy

$$\mu a = \frac{1}{2}\frac{\bar{q}}{\omega_0}\sin\theta, \tag{3.28}$$

$$\sigma - \frac{3}{8}\frac{P_3}{\omega_0}a^2 = -\frac{1}{2}\frac{\bar{q}}{\omega_0}\cos\theta. \tag{3.29}$$

The equation for the frequency response is presented as:

$$\left[\left(\sigma - \frac{3}{8}\frac{P_3}{\omega_0}a^2\right)^2 + \mu^2\right]a^2 = \frac{\bar{q}^2}{4\omega_0^2}. \tag{3.30}$$

Substituting Eq. (3.26) into Eq. (3.30) and then substituting that result into Eqs. (3.28) and (3.29), one can obtain:

$$w = a\cos(\omega_0 t + \varepsilon\sigma t - \theta) + O(\varepsilon). \tag{3.31}$$

With this, the amplitude response (the magnification factor) can be obtained as:

$$M = \frac{a}{|\bar{q}|} = \frac{1}{2\omega_0\sqrt{\left(\sigma - \frac{3}{8}\frac{P_3}{\omega_0}a^2\right)^2 + \mu^2}}. \tag{3.32}$$

Similar to the case of the linear oscillator, the maximum value of the magnification factor can be obtained from

$$\frac{\mathrm{d}M}{\mathrm{d}\Omega} = 0, \qquad \frac{\mathrm{d}^2M}{\mathrm{d}\Omega^2} = 0. \tag{3.33}$$

Equation (3.33) with respect to Ω yields:

$$\frac{1}{32}a\left(3P_3a^2 - 8\Omega - 8\right)\left(3P_3\frac{\mathrm{d}a}{\mathrm{d}\Omega} - 4\right) + \left(\mu^2 + (\Omega - 1 - 3P_3a^2)^2\right)\frac{\mathrm{d}a}{\mathrm{d}\Omega} = 0 \tag{3.34}$$

which can be solved for $\frac{\mathrm{d}a}{\mathrm{d}\Omega}$ as:

$$\frac{\mathrm{d}a}{\mathrm{d}\Omega} = \frac{8a\left(3P_3a^2 - 8\Omega - 8\right)}{27P_3^2a^4 - 96(\Omega-1)P_3a^2 + 64\left(\mu^2 + (\Omega-1)^2\right)}. \tag{3.35}$$

This derivative vanishes (and so does $\frac{\mathrm{d}M}{\mathrm{d}\Omega}$) when:

$$\left(3P_3a^2 - 8\Omega - 8\right) = 0 \implies a_p = \sqrt{\frac{8(\Omega-1)}{3P_3}}. \tag{3.36}$$

To find the values of the critical points Ω_1 and Ω_2, which correspond to vertical tangencies of the response curve, where $\frac{\mathrm{d}M}{\mathrm{d}\Omega} = 0$:

$$27P_3^2a^4 - 96(\Omega-1)P_3a^2 + 64\left(\mu^2 + (\Omega-1)^2\right). \tag{3.37}$$

This above condition is found by equating the denominator of Eq. (3.36) to zero, and the roots of this equation give Ω_1 and Ω_2 can be expressed as:

$$\Omega_{1,2} = \frac{1}{8}\left(8 + 6P_3a^2 - \sqrt{9P_3^2a^4 - 64\mu^2}\right). \tag{3.38}$$

4. Numerical results and discussion

In this section, the vibration behavior of a nanobeam made of piezoelectric material in a magnetic field is studied (Table 1 and Table 2).

Table 1. Material constants for MEV $BaTiO_3$-$CoFe_2O_4$ composite.

Properties	$BaTiO_3$-$CoFe_2O_4$
C_{11} [GPa]	154.81
C_{55}	44.2
e_{31} [$\mathrm{C\cdot m^{-2}}$]	−7.54
e_{15}	5.8
q_{31} [N/(A · m)]	89.23
q_{15}	275
χ_{11} [10^{-9} $\mathrm{C^2\cdot m^{-2}\cdot N^{-1}}$]	5.64
χ_{33}	5.95
λ_{11} [10^{-4} $\mathrm{N\cdot s^2\cdot C^{-2}}$]	−297
λ_{33}	650.3
d_{11} [10^{-12} (N · s)/(V · C)]	5.36
d_{33}	2752.56
ρ [$\mathrm{kg\cdot m^{-3}}$]	5550

Table 2. The properties of a multiscale composite shell (SHEN *et al.* [35]; SAHMANI and AGHDAM [36]).

Carbon (fiber)	Epoxy (matrix)	Carbon nanotube	Graphene platelet
E_{11}^f [GPa] $= 233.05$	$v^m = 0.3$	E^{cn} [GPa] $= 640[1 - 0.0005\Delta T]$	E^{gpl} [GPa] $= [3.52 - 0.0034T]$
E_{11}^f [GPa] $= 23.1$	ρ^m [kg $\cdot$ m] $= 1200$	d^{cn} [m] $= 1.4 \cdot 10^{-9}$	d^{gpl} [m] $= 14.76 \cdot 10^{-9}$
G_{12}^f [GPa] $= 8.96$	E^m [GPa] $= [3.51 - 0.0034T + 0.142H]$	t^{cn} [m] $= 0.34 \cdot 10^{-9}$	t^{gpl} [m] $= 14.77 \cdot 10^{-9}$
$v^f = 0.6$	α_m [K^{-1}] $= 45(1 + 0.001T) \cdot 10^{-6}$	l^{cn} [m] $= 25 \cdot 10^{-6}$	h^{gpl} [m] $= 0.188 \cdot 10^{-9}$
ρ^f [kg/m^3] $= 0.2$	β [wt%$^{-1}$] $= 2.68 \cdot 10^{-3}$	l^{cn} [m] $= 0.25 \cdot 10^{-9}$	$\vartheta_{12} = 0.177$
α_{11} [K^{-1}] $= -0.54 \cdot 10^{-6}$		$\vartheta_{12} = 0.33$	ρ^{gpl} [kg/m^3] $= 4118$
α_{22} [K^{-1}] $= 10.8 \cdot 10^{-6}$		ρ^{cn} [kg/m^3] $= 1350$	α_{11} [K^{-1}] $= -0.9 \cdot 10^{-6}$
		α_{11} [K^{-1}] $= 4.5361 \cdot 10^{-6}$	α_{22} [K^{-1}] $= -0.95 \cdot 10^{-6}$
		α_{22} [K^{-1}] $= 4.6677 \cdot 10^{-6}$	

The validity of the present study is proved by comparing the frequencies of this model with those of Ebrahimi and Salari [32] for various nonlocal parameters as presented in Table 3. Also, the dimensionless frequency and dimensionless viscoelastic parameters with $C_{11} = E$ and $I = h^3/12$ are adopted as:

$$\overline{\omega} = \omega L^2 \sqrt{\frac{\rho A}{EI}}, \qquad K_w = k_w \frac{L^4}{EI}, \qquad K_p = k_p \frac{L^2}{EI}, \qquad C = c_d \frac{L^2}{\sqrt{\rho AEI}}, \qquad \eta = \frac{g_0}{L^2}\sqrt{\frac{EI}{\rho A}}. \tag{4.1}$$

Table 3. Comparison of the non-dimensional frequency of undamped S–S nanobeam.

L/h	P	ΔT	μ [nm^2]	Non-dimensional frequency	
				Ebrahimi and Salari [32]	Present
20	0	0	0	9.6468	9.65189
			1	9.1859	9.19080
			2	8.7825	8.78720
			3	8.4254	8.42995

Figure 2 demonstrates the second resonance of the clamped FG beam, occurring near the first mode, while considering both strain gradient and nonlocal parameters. Notably, the right branches in the depicted figures exhibit points of vertical tangency, leading to a jump phenomenon frequently observed in nonlinear vibratory systems. Figure 3 displays the phase angle characteristics of the clamped FG beam near the first mode, incorporating strain gradient and nonlocal parameters. Notably, the right branches in the depicted figures reveal points of vertical tangency, resulting in a common jump phenomenon observed

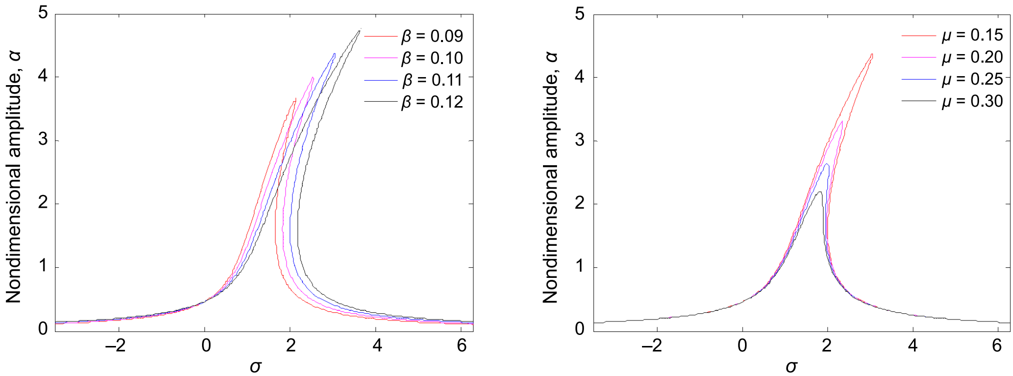

Fig. 2. Plots of dimensionless amplitude vs. stress field for various strain gradient and nonlocal parameters ($l = 2\pi$, $F0 = 20$).

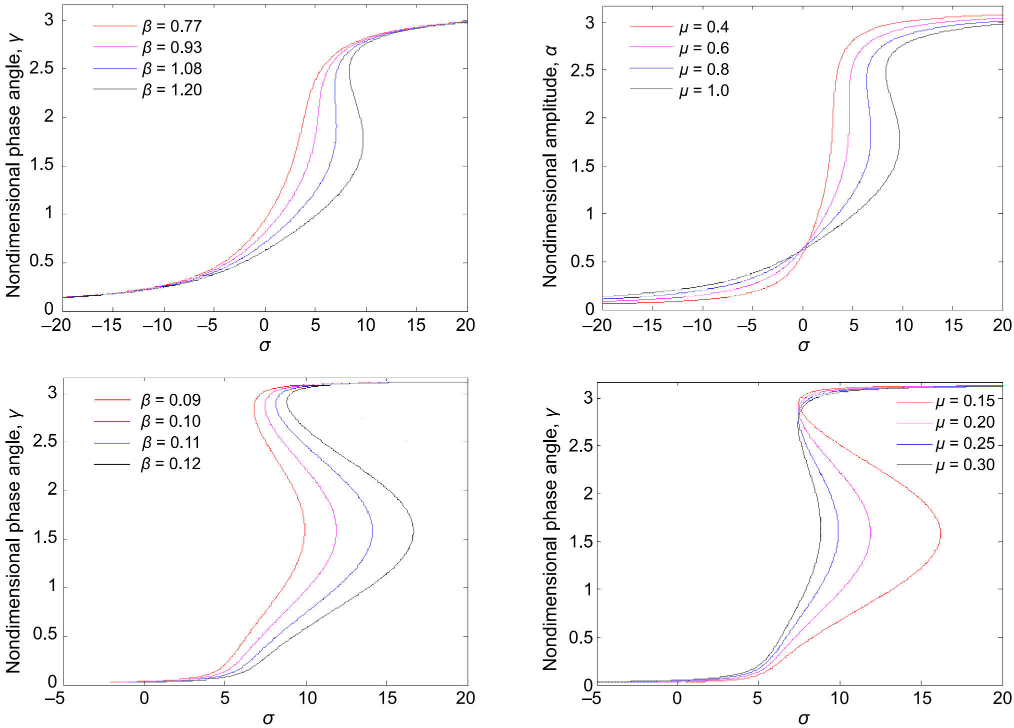

FIG. 3. Plots of dimensionless phase angle vs. stress field for various strain gradient and nonlocal parameters ($l = 2\pi$, $F0 = 20$).

in nonlinear vibratory systems. Notably, within the 1/2 subharmonic parametric resonance, there are nine dynamic buckling patterns, and all curves on the transition set can be described as either straight lines or quadratic curves. Figure 4 showcases the amplitude behavior of the clamped FG beam around the

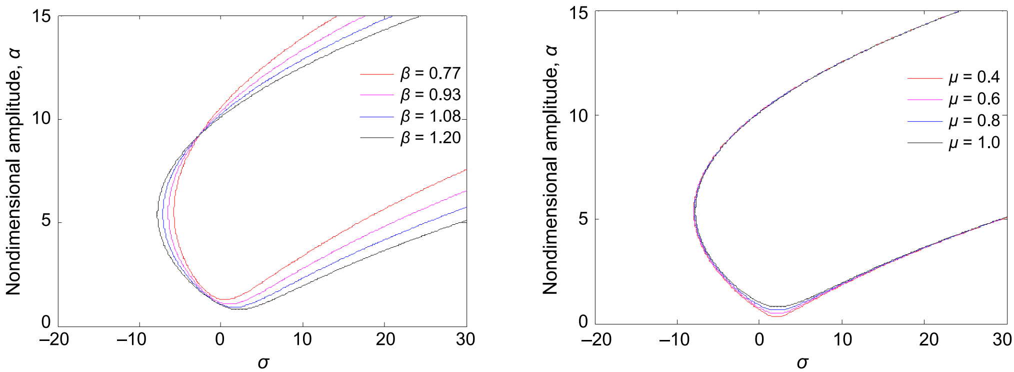

FIG. 4. Plots of dimensionless amplitude vs. stress field for various strain gradient and nonlocal parameters.

first mode, considering both strain gradient and nonlocal parameters. As evident from the depicted figures, the right branches display points of vertical tangency, leading to a typical jump phenomenon observed in nonlinear vibratory systems.

5. Conclusions

This article investigated the forced harmonic vibration of a magneto-electro-viscoelastic nanobeam resting on a viscoelastic medium, based on a nonlocal refined beam theory with various boundary conditions. According to the nonlocal strain gradient theory, the governing equations are obtained using Hamilton's principle and solved implementing an analytical solution. Then, nondimensional amplitude and phase angles are studied over stress fields and the key findings are as follows:

- Once the nonlocal parameter is increased, a wave amplitude becomes smaller.
- The higher strain gradient parameter value amplifies the amplitude and reduces the phase angle.
- The phase angle is affected by both the nonlocal parameter and the load factors.
- An increase in the stress field strength leads to a decrease of the phase angle's rigidity.
- By amplifying the stress field strength and nonlocal values, the non-dimensional amplitude undergoes a decrease.
- It is noticed that the curves on the transition set are straight lines or quadratic.

Appendix

$$M_{11} = I_0 \left(\mu\overline{X}_{13} - \overline{X}_{11}\right),$$
$$M_{12} = I_1 \left(\overline{X}_{11} - \mu\overline{X}_{13}\right),$$
$$M_{13} = I_2 \left(\overline{X}_{11} - \mu\overline{X}_{13}\right),$$
$$M_{21} = I_1 \left(\mu\overline{X}_{40} - \overline{X}_{20}\right),$$
$$M_{22} = I_0 \left(\mu\overline{X}_{20} - \overline{X}_{00}\right) + I_4 \left(\overline{X}_{20} - \mu\overline{X}_{40}\right),$$
$$M_{23} = I_0 \left(\mu\overline{X}_{20} - \overline{X}_{00}\right) + I_3 \left(\overline{X}_{20} - \mu\overline{X}_{40}\right),$$
$$M_{31} = I_2 \left(\mu\overline{X}_{40} - \overline{X}_{20}\right),$$
$$M_{32} = I_0 \left(\mu\overline{X}_{20} - \overline{X}_{00}\right) + I_3 \left(\overline{X}_{20} - \mu\overline{X}_{40}\right),$$

$$M_{33} = I_0 \left(\mu\overline{X}_{20} - \overline{X}_{00}\right) + I_5 \left(\overline{X}_{20} - \mu\overline{X}_{40}\right),$$

$$C_{11} = ig_0 J_{11} \left(\lambda\overline{X}_{15} - \overline{X}_{13}\right),$$

$$C_{12} = ig_0 J_{11}^{z} \left(\overline{X}_{13} - \lambda\overline{X}_{15}\right),$$

$$C_{13} = ig_0 J_{11}^{f} \left(\overline{X}_{13} - \lambda\overline{X}_{15}\right),$$

$$C_{21} = ig_0 J_{11}^{z} \left(\lambda\overline{X}_{60} - \overline{X}_{40}\right),$$

$$C_{22} = i \left(\overline{X}_{00} - \mu\overline{X}_{20}\right) c_d + ig_0 J_{11}^{zz} \left(\overline{X}_{40} - \lambda\overline{X}_{60}\right),$$

$$C_{23} = i \left(\overline{X}_{00} - \mu\overline{X}_{20}\right) c_d + ig_0 J_{11}^{zf} \left(\overline{X}_{40} - \lambda\overline{X}_{60}\right),$$

$$C_{31} = ig_0 J_{11}^{f} \left(\lambda\overline{X}_{60} - \overline{X}_{40}\right),$$

$$C_{32} = i \left(\overline{X}_{00} - \mu\overline{X}_{20}\right) c_d + ig_0 J_{11}^{zf} \left(\overline{X}_{40} - \lambda\overline{X}_{60}\right),$$

$$C_{33} = i \left(\overline{X}_{00} - \mu\overline{X}_{20}\right) c_d + ig_0 J_{11}^{ff} \left(\overline{X}_{40} - \lambda\overline{X}_{60}\right) + ig_0 K_{55} \left(\lambda\overline{X}_{40} - \overline{X}_{20}\right),$$

$$k_{11} = J_{11} \left(\lambda\overline{X}_{15} - \overline{X}_{13}\right),$$

$$k_{12} = J_{11}^{z} \left(\overline{X}_{13} - \lambda\overline{X}_{15}\right),$$

$$k_{13} = J_{11}^{f} \left(\overline{X}_{13} - \lambda\overline{X}_{15}\right),$$

$$k_{14} = K_{31}^{e} \left(\lambda\overline{X}_{13} - \overline{X}_{11}\right),$$

$$k_{15} = K_{31}^{m} \left(\lambda\overline{X}_{13} - \overline{X}_{11}\right),$$

$$k_{21} = J_{11}^{z} \left(\lambda\overline{X}_{60} - \overline{X}_{40}\right),$$

$$k_{22} = \left(N^E + N^H\right) \left(\overline{X}_{20} - \mu\overline{X}_{40}\right) + k_w \left(\overline{X}_{00} - \mu\overline{X}_{20}\right) + k_p \left(\mu\overline{X}_{40} - \overline{X}_{20}\right) + J_{11}^{zz} \left(\overline{X}_{40} - \lambda\overline{X}_{60}\right),$$

$$k_{23} = \left(N^E + N^H\right) \left(\overline{X}_{20} - \mu\overline{X}_{40}\right) + k_w \left(\overline{X}_{00} - \mu\overline{X}_{20}\right) + k_p \left(\mu\overline{X}_{40} - \overline{X}_{20}\right) + J_{11}^{zf} \left(\overline{X}_{40} - \lambda\overline{X}_{60}\right),$$

$$k_{24} = X_{31}^{e} \left(\lambda\overline{X}_{40} - \overline{X}_{20}\right),$$

$$k_{25} = X_{31}^{m} \left(\lambda\overline{X}_{40} - \overline{X}_{20}\right),$$

$$k_{31} = J_{11}^{f} \left(\lambda\overline{X}_{60} - \overline{X}_{40}\right),$$

$$k_{32} = \left(N^E + N^H\right) \left(\overline{X}_{20} - \mu\overline{X}_{40}\right) + k_w \left(\overline{X}_{00} - \mu\overline{X}_{20}\right) + k_p \left(\mu\overline{X}_{40} - \overline{X}_{20}\right) + J_{11}^{zf} \left(\overline{X}_{40} - \lambda\overline{X}_{60}\right),$$

$$k_{33} = \left(N^E + N^H\right)\left(\overline{X}_{20} - \mu\overline{X}_{40}\right) + k_w\left(\overline{X}_{00} - \mu\overline{X}_{20}\right) + k_p\left(\mu\overline{X}_{40} - \overline{X}_{20}\right) + K_{55}\left(\lambda\overline{X}_{40} - \overline{X}_{20}\right) + J_{11}^{ff}\left(\overline{X}_{40} - \lambda\overline{X}_{60}\right),$$

$$k_{34} = \left(Y_{31}^e - X_{15}\right)\left(\lambda\overline{X}_{40} - \overline{X}_{20}\right),$$

$$k_{35} = \left(Y_{31}^m - Y_{15}\right)\left(\lambda\overline{X}_{40} - \overline{X}_{20}\right),$$

$$k_{41} = K_{31}^e\left(\overline{X}_{20} - \lambda\overline{X}_{40}\right),$$

$$k_{42} = X_{31}^e\left(\lambda\overline{X}_{40} - \overline{X}_{20}\right),$$

$$k_{43} = \left(X_{15} - Y_{31}^e\right)\left(\overline{X}_{20} - \lambda\overline{X}_{40}\right),$$

$$k_{44} = X_{11}\left(\overline{X}_{20} - \lambda\overline{X}_{40}\right) + X_{33}\left(\lambda\overline{X}_{20} - \overline{X}_{00}\right),$$

$$k_{45} = Y_{11}\left(\overline{X}_{20} - \lambda\overline{X}_{40}\right) + Y_{33}\left(\lambda\overline{X}_{20} - \overline{X}_{00}\right),$$

$$k_{51} = K_{31}^m\left(\overline{X}_{20} - \lambda\overline{X}_{40}\right),$$

$$k_{52} = X_{31}^m\left(\lambda\overline{X}_{40} - \overline{X}_{20}\right),$$

$$k_{53} = \left(Y_{15} - Y_{31}^m\right)\left(\overline{X}_{20} - \lambda\overline{X}_{40}\right),$$

$$k_{54} = Y_{11}\left(\overline{X}_{20} - \lambda\overline{X}_{40}\right) + Y_{33}\left(\lambda\overline{X}_{20} - \overline{X}_{00}\right),$$

$$k_{55} = K_{11}\left(\overline{X}_{20} - \lambda\overline{X}_{40}\right) + K_{33}\left(\lambda\overline{X}_{20} - \overline{X}_{00}\right),$$

$$F_{33}^e = F_{33}^m = 0.$$

References

1. Van Den Boomgaard J., Terrell D.R., Born R.A.J., Giller H.F.J.I., An in situ grown eutectic magnetoelectric composite material, *Journal of Materials Science*, **9**: 1705–1709, 1974, doi: 10.1007/BF00540770.

2. Zheng H., Wang J., Lofland S.E., Ma Z., Mohaddes-Ardabili L., Zhao T., Salamanca-Riba L., Shinde S.R., Ogale S.B., Bai F., Viehland D., Jia Y., Schlom D.G., Wuttig M., Roytburd A., Ramesh R., Multiferroic $BaTiO_3$-$CoFe_2O_4$ nanostructures, *Science*, **303** (5658): 661–663, 2004, doi: 10.1126/science.1094207.

3. Martin L.W., Crane S.P., Chu Y.H., Holcom M.B., Gajek M., Huijben M., Yang C.H., Balke N., Ramesh R., Multiferroics and magnetoelectrics: thin films and nanostructures, *Journal of Physics: Condensed Matter*, **20**(43): 434220, 2008, doi: 10.1088/0953-8984/20/43/434220.

4. Wang Y., Hu J.M., Lin Y.H., Nan C.W., Multiferroic magnetoelectric composite nanostructures, *NPG Asia Materials*, **2**: 61–68, 2010, doi: 10.1038/asiamat.2010.32.

5. Prashanthi K., Shaibani P.M., Sohrabi A., Natarajan T.S., Thundat T., Nanoscale magnetoelectric coupling in multiferroic $BiFeO_3$ nanowires, *Physica Status Solidi RRL*, **6**: 244–246, 2012, doi: 10.1002/pssr.201206135.

6. Eringen A., Mechanics of micromorphic continua, [in] E. Kröner (Ed.), *Mechanics of Generalized Continua*, IUTAM Symposia, Springer, Berlin, Heidelberg, 1968, pp. 18–35, doi: 10.1007/978-3-662-30257-6_2.

7. Eringen A., Nonlocal polar elastic continua, *International Journal of Engineering Science*, **10**(1): 1–16, 1972, doi: 10.1016/0020-7225(72)90070-5.

8. Eringen A., Nonlocal micropolar field theory, [In:] *Continuum Physics*, Eringen A.C. (Ed.), Academic Press, New York, 1976.

9. Eringen A., *Nonlocal Continuum Field Theories*, Springer, New York, 2002.

10. Eringen A., Nonlocal continuum mechanics based on distributions, *International Journal of Engineering Science*, **44**(3–4): 141–147, 2006, doi: 10.1016/j.ijengsci.2005.11.002.

11. Eringen A.C., On differential equations of nonlocal elasticity and solutions of screw dislocation and surface waves, *Journal of Applied Physics*, **54**(9): 4703–4710, 1983, doi: 10.1063/1.332803.

12. Li L., Hu Y., Ling L., Flexural wave propagation in small-scaled functionally graded beams via a nonlocal strain gradient theory, *Composite Structures*, **133**: 1079–1092, 2015, doi: 10.1016/j.compstruct.2015.08.014.

13. Lam D.C.C., Yang F., Chong A.C.M., Wang J., Tong P., Experiments and theory in strain gradient elasticity, *Journal of the Mechanics and Physics of Solids*, **51**(8): 1477–1508, 2003, doi: 10.1016/S0022-5096(03)00053-X.

14. Peddieson J., Buchanan G.R., McNitt R.P., Application of nonlocal continuum models to nanotechnology, *International Journal of Engineering Science*, **41**(3–5): 305–312, 2003, doi: 10.1016/S0020-7225(02)00210-0.

15. Zenkour A.M., Sobhy M., Nonlocal elasticity theory for thermal buckling of nanoplates lying on Winkler-Pasternak elastic substrate medium, *Physica E: Low-dimensional Systems and Nanostructures*, **53**: 251–259, 2013, doi: 10.1016/j.physe.2013.04.022.

16. Wang Q., Wave propagation in carbon nanotubes via nonlocal continuum mechanics, *Journal of Applied Physics*, **98**: 124301, 2005, doi: 10.1063/1.2141648.

17. Wang C.M., Kitipornchai S., Lim C.W., Eisenberger M., Beam bending solutions based on nonlocal Timoshenko beam theory, *Journal of Engineering Mechanics*, **134**(6): 475–481, 2008, doi: 10.1061/(ASCE)0733-9399(2008)134:6(475).

18. Civalek O., Demir C., Bending analysis of microtubules using nonlocal Euler-Bernoulli beam theory, *Applied Mathematical Modelling*, **35**(5): 2053–2067, 2011, doi: 10.1016/j.apm.2010.11.004.

19. Murmu T., Pradhan S.C., Buckling analysis of a single-walled carbon nanotube embedded in an elastic medium based on nonlocal elasticity and Timoshenko beam theory and using DQM, *Physica E: Low-dimensional Systems and Nanostructures*, **41**(7): 1232–1239, 2009, doi: 10.1016/j.physe.2009.02.004.

20. Yang J., Ke L.L., Kitipornchai S., Nonlinear free vibration of single-walled carbon nanotubes using nonlocal Timoshenko beam theory, *Physica E: Low-dimensional Systems and Nanostructures*, **42**(5): 1727–1735, 2010, doi: 10.1016/j.physe.2010.01.035.

21. Roque C.M.C., Ferreira A.J.M., Reddy J.N., Analysis of Timoshenko nanobeams with a nonlocal formulation and meshless method, *International Journal of Engineering Science*, **49**(9), 976–984, 2011, doi: 10.1016/j.ijengsci.2011.05.010.

22. Şimşek M., Yurtcu H.H., Analytical solutions for bending and buckling of functionally graded nanobeams based on the nonlocal Timoshenko beam theory, *Composite Structures*, **97**: 378–386, 2013, doi: 10.1016/j.compstruct.2012.10.038.

23. Arefi M., Zenkour A.M., A simplified shear and normal deformations nonlocal theory for bending of functionally graded piezomagnetic sandwich nanobeams in magneto-thermo-electric environment, *Journal of Sandwich Structures & Materials*, **18**(5): 624–651, 2016, doi: 10.1177/1099636216652581.

24. Selvamani R., Loganathan R., Ebrahimi F., Nonlocal state-space strain gradient approach to the vibration of piezoelectric functionally graded nanobeam, *Engineering Transactions*, **70**(4): 319–338, 2022, doi: 10.24423/EngTrans.2242.20221020.

25. Selvamani R., Mahaveer Sreejayan M., Ebrahimi F., Static stability analysis of mass sensors consisting of hygro-thermally activated graphene sheets using a nonlocal strain gradient theory, *Engineering Transactions*, **68**(3): 269–295, 2020, doi: 10.24423/EngTrans.1187.20200904.

26. Selvamani R., Makinde O.D., Influence of rotation on transversely isotropic piezoelectric rod coated with a thin film, *Engineering Transactions*, **66**(3): 211–227, 2018, doi: 10.24423/EngTrans.859.20180726.

27. Ebrahimi F., Jafari A., Selvamani R., Thermal buckling analysis of magneto electro elastic porous FG beam in thermal environment, *Advances in Nano Research*, **8**(1): 83–94, 2020, doi: 10.12989/anr.2020.8.1.083.

28. Ebrahimi F., Karimiasl M., Selvamani R., Bending analysis of magneto-electro piezoelectric nanobeams system under hygro-thermal loading, *Advances in Nano Research*, **8**(3): 203–214, 2020, doi: 10.12989/anr.2020.8.3.203.

29. Ke L.L., Wang Y.S., Yang J., Kitipornchai S., Free vibration of size-dependent magneto-electro-elastic nanoplates based on the nonlocal theory, *Acta Mechanica Sinica*, **30**(4): 516–525, 2014, doi: 10.1007/s10409-014-0072-3.

30. Ke L.L., Wang Y.S., Free vibration of size-dependent magneto-electro-elastic nanobeams based on the nonlocal theory, *Physica E: Low-dimensional Systems and Nanostructures*, **63**: 52–61, 2014, doi: 10.1016/j.physe.2014.05.002.

31. Mantari J.L., Bonilla E.M., Soares C.G., A new tangential-exponential higher order shear deformation theory for advanced composite plates, *Composites Part B: Engineering*, **60**: 319–328, 2014, doi: 10.1016/j.compositesb.2013.12.001.

32. Ebrahimi F., Salari E., Effect of various thermal loadings on buckling and vibrational characteristics of nonlocal temperature-dependent FG nanobeams, *Mechanics of Advanced Materials and Structures*, **23**(12): 1379–1397, 2016, doi: 10.1080/15376494.2015.1091524.

33. Ebrahimi F., Kokaba M., Shaghaghi G., Selvamani R., Dynamic characteristics of hygro-magneto-thermo-electrical nanobeam with non-ideal boundary conditions, *Advances in Nano Research*, **8**(2): 169–182, 2020, doi: 10.12989/ANR.2020.8.2.169.

34. Ebrahimi F., Hamed Hosseini S., Selvamani R., Thermo-electro-elastic nonlinear stability analysis of viscoelastic double-piezo nanoplates under magnetic field, *Structural Engineering and Mechanics, An International Journal*, **73**(5): 565–584, 2020, doi: 10.12989/sem.2020.73.5.565.

35. Shen Y., Hu Y., Chen W., Wang J., Guan Y., Du J., Zhang X., Ma J., Li M., Lin Y., Chen L.Q., Nan C.W., Modulation of topological structure induces ultrahigh energy density of graphene/Ba0.6Sr0.4TiO3 nanofiber/polymer nanocomposites, *Nano Energy*, **18**: 176–186, 2015, doi: 10.1016/j.nanoen.2015.10.003.

36. Sahmani S., Aghdam M.M., Nonlocal strain gradient beam model for nonlinear vibration of prebuckled and postbuckled multilayer functionally graded GPLRC nanobeams, *Composite Structures*, **179**: 77–88, 2017, doi: 10.1016/j.compstruct.2017.07.064.

Received February 1, 2023; accepted version September 22, 2023.